Temperature- and frequency-dependent optical properties of ultrathin Au films

Tobby Brandt, Martin Hövel, Bruno Gompf, and Martin Dressel
1. Physikalisches Institut, Universität Stuttgart, Pfaffenwaldring 57, 70550 Stuttgart Germany
(Received 20 August 2008; revised manuscript received 15 October 2008; published 7 November 2008)

While the optical properties of thin metal films are well understood in the visible and near-infrared range, little has been done in the midinfrared and far-infrared region. Here we investigate ultrathin gold films prepared on Si(111)(7×7) in UHV by measuring in the frequency range between 500 and 7000 cm^{-1} and for temperatures between 300 and 5 K. The nominal thickness of the gold layers ranges between one monolayer and 9 nm. The frequency and temperature dependences of the thicker films can be well described by the Drude model of a metal when taking into account classical size effects due to surface scattering. The films below the percolation threshold exhibit a nonmetallic behavior; the reflection increases with frequency and decreases with temperature. The frequency dependence can partly be described by a generalized Drude model. The temperature dependence does not follow a simple activation process. For monolayers we observe a transition between surface states around 1100 cm^{-1}.

DOI: 10.1103/PhysRevB.78.205409 PACS number(s): 78.20.−e, 71.30.+h, 73.25.+i, 73.63.Bd

I. INTRODUCTION

The optical properties of thick metal films in the infrared spectral range are similar to bulk material[1] and can be well described by the Drude model, except that interface scattering becomes increasingly important as the thickness d is reduced below the mean-free path ℓ, which is approximately 40 nm for the example of gold.[2] For extremely thin films not only the scattering rate increases, but in addition they exhibit a drop of the effective carrier density, seen in a reduced plasma frequency;[3,4] this can be explained by a modified band-structure and dipole layers at the interfaces. When the film thickness shrinks even further, normally a metal-to-insulator transition is observed in the electrical transport, known as the percolation threshold.[5,6] The discontinuous film morphology does not only affect the dc resistivity but also the optical properties. Above the percolation threshold, the infrared reflectivity decreases with increasing frequency, it becomes nearly frequency independent at the threshold, and finally increases with frequency below the percolation threshold.[7]

During the deposition process, nanometer-sized metal clusters are created through nucleation and growth. Above a critical thickness d_c, these islands coalesce to form a conducting network. In principle, one can consider semicontinuous metal films as composition of metallic particles embedded in an insulating matrix and try to describe their optical properties with effective-medium theories (EMA).[8,9] However, it was shown that EMA models fail to predict the dielectric behavior of discontinuous films,[10–12] mainly because they neglect interface effects.

The temperature-dependent dc resistivity of thin metal films above the percolation threshold contains contributions from regular phonon scattering, but in addition from grain boundary and surface scattering. Both processes lead to a thickness-dependent shift of the (temperature-dependent) resistivity to higher values as the films get thinner. The overall behavior, however, does not change; at higher temperatures, $\rho(T)$ exhibits a linear dependence, while at lower temperatures a temperature-independent residual resistance remains.[13,14] For discontinuous metal films (below the percolation threshold) Hill found an activated dc transport with an activation energy of less than 100 meV for gold films on glass.[15]

To the best of our knowledge, there exist no temperature-dependent infrared investigations on ultrathin metal films around the percolation threshold. In order to improve our understanding of these films, we have carried out low-temperature infrared optical studies on gold layers with a nominal thickness varying between one monolayer and 9 nm.

II. EXPERIMENTS

Thin Au films were prepared by an electron-beam heated effusion cell on clean Si(111)(7×7) surfaces in UHV at a base pressure below 10^{-10} mbar. During evaporation the samples were at room temperature and the evaporation rate was about 0.1 nm/min. The film thickness was monitored by a quartz microbalance. Additionally the clean surface and the monolayers were characterized by low-energy electron diffraction (LEED). Whereas the clean Si(111) surface exhibits the well-known (7×7) reconstruction, one monolayer of Au on Si leads to the formation of a well-ordered Si(111)-Au(6×6) reconstruction.[16]

After preparation, the films were transferred to an optical UHV cryostat without breaking the vacuum. The cryostat has one ZnSe window for reflection measurements in nearly normal incidence and is attached to a Bruker IFS 113v Fourier-transform infrared spectrometer (FTIR). The investigations were performed in the midinfrared and near-infrared spectral range between 500 and 7000 cm^{-1}, employing a nitrogen cooled mercury-cadmium-telluride (MCT) detector. The spectra were recorded with a resolution of 8 cm^{-1} and in each case 128 spectra were averaged. The He cold-finger cryostat allows us to measure at temperatures down to 5 K. As reference the same sample was used but coated with an *in situ* evaporated thick gold film. In this way an accuracy in the reflection measurements better than 1% can be achieved.

III. RESULTS AND ANALYSIS

The results can be divided in three clearly distinguishable regimes: the continuous films in the thickness range above 4

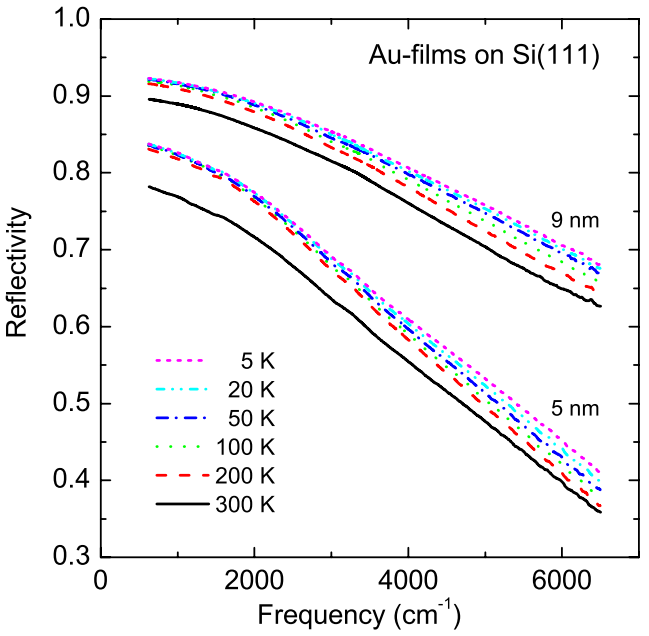

FIG. 1. (Color online) Frequency dependent reflectivity of thin Au films above the percolation threshold measured at various temperatures as indicated. For the 9 nm and the 5 nm thick films the optical behavior can be fitted by a Drude model when classical size effects are considered.

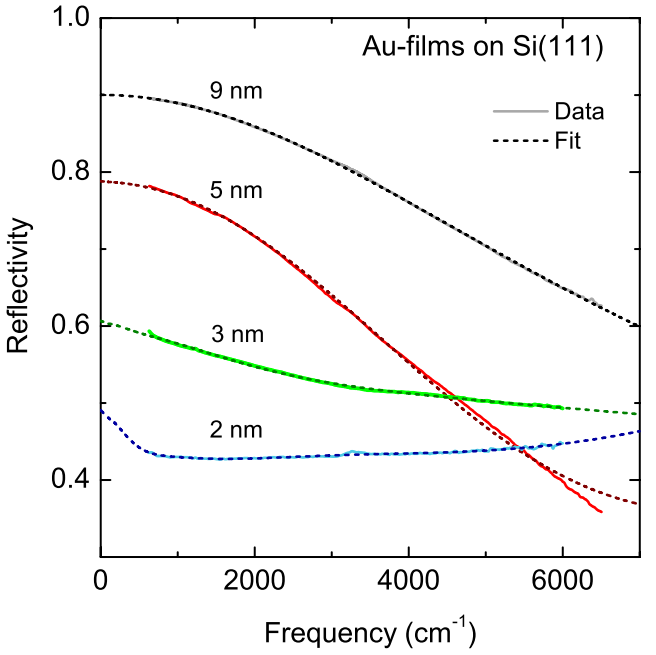

FIG. 2. (Color online) Frequency-dependent reflectivity of thin Au-films on Si(111) at 300 K together with the corresponding fits. The 9 nm and the 5 nm films can be fitted purely by the Drude model with the parameters listed in Table I. For the 3 nm and the 2 nm film an additional Lorentz oscillator at higher frequencies is needed for reasonable description.

nm, the films close to the percolation threshold around 2 nm, and the monolayer range.

A. Thick films above the percolation threshold

Figure 1 shows the temperature-dependent reflectivity spectra for a 9 nm and a 5 nm thick films. The reflectivity decreases with increasing frequency and becomes better as the temperature is lowered; this behavior corresponds to normal metals and can be fitted by the Drude model,[17] in which the real part of the conductivity is given by

$$\sigma_1(\omega) = \frac{\omega_p^2 \tau}{4\pi} \frac{1}{1+\omega^2\tau^2}; \tag{1}$$

here ω_p is the plasma frequency, and τ denotes the scattering time. This fit yields the plasma frequency ω_p and scattering rate $\gamma = 1/(2\pi c\tau)$ as listed in Table I.

In Fig. 2 a comparison between the 300 K measurements and the calculated reflectivity for the layer system: fitted Drude-metal/Si is additionally shown. Included in Fig. 2 as well as in Table I are also the Drude parameters for the 3 nm and the 2 nm films, although these films cannot be described by a pure Drude model. For there description an additional Lorentz oscillator[17] at higher frequencies is needed

$$\sigma_1(\omega) = \frac{\omega_p^2 \tau}{4\pi} \frac{\omega^2/\tau^2}{(\omega_0^2-\omega^2)^2+\omega^2/\tau^2}; \tag{2}$$

with ω_0 the center frequency. The broad oscillator at higher frequencies reduces the plasma frequency in the Drude term, which together with the higher scattering rate leads to the lower reflectivity at lower frequencies for these films (see

TABLE I. Room temperature properties of thin metal films obtained from a Drude fit of the optical data. $\sigma_1(\omega \to 0)$ corresponds to the dc extrapolation of the optical conductivity, ω_p is the plasma frequency and $\gamma = 1/(2\pi c\tau)$ denotes the scattering rate. For the accurate description of the 3 and 2 nm films, additionally a Lorentz oscillator is needed with the center frequency ω_0 and the width γ.

	Drude components			Lorentz oscillator		
Film thickness (nm)	$\sigma_1(\omega \to 0)$ (10^4 Ω^{-1} cm^{-1})	$\omega_p/2\pi c$ (10^4 cm^{-1})	γ (cm^{-1})	$\omega_0/2\pi c$ (cm^{-1})	$\omega_p/2\pi c$ (10^4 cm^{-1})	γ (cm^{-1})
Bulk	40.9	7.27	215			
9	10.2	7.13	831			
5	7.0	7.81	1448			
3	3.8	6.19	1696	5380	13.21	18670
2	1.9	4.95	2165	4180	7.41	8240

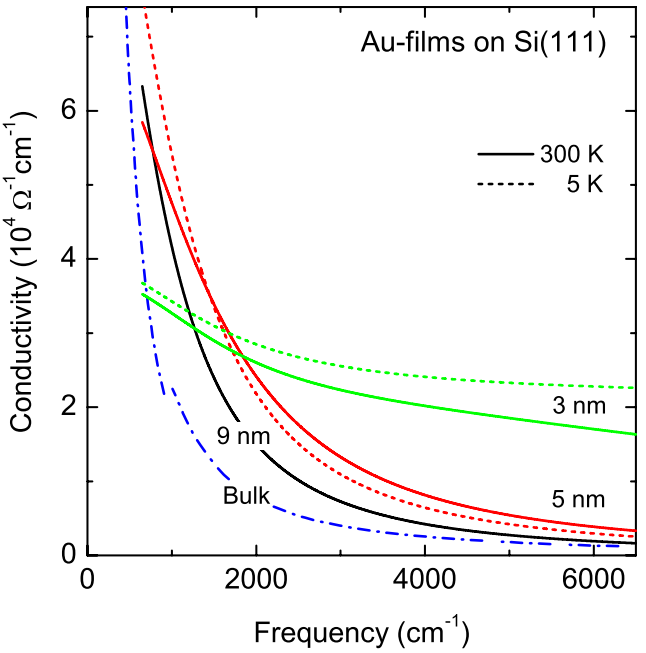

FIG. 3. (Color online) Optical conductivity of thin gold films on Si(111) obtained from reflectivity measurements on films with a thickness of d=3, 5, and 9 nm, as indicated. The solid lines correspond to the room-temperature data, the dotted lines to T=5 K. In addition the bulk data (dashed dotted line) are shown as obtained from Refs. 1 and 17.

Fig. 2). The 5 nm and 9 nm layer exhibit plasma frequencies, which are close to that of bulk Au.[1] As for bulk metals, the plasma frequency in all films is temperature independent. The higher scattering rate for thinner films is a typical size effect; thinner films exhibit a stronger surface scattering due to a larger surface-to-volume fraction.

With the Eqs. (1) and (2) and the parameters listed in Table I the corresponding conductivity of the films can be calculated (Fig. 3). By comparison of the 5 nm film with the 9 nm film, which both can be described by a pure Drude, it becomes obvious that an increase in scattering rate for thin films leads to an enhanced conductivity in the midinfrared range. For the two thinner films the strongly enhanced midinfrared conductivity is mainly due to the Lorentz oscillator [Eq. (2)] as can be seen in Fig. 4, where the different contributions to the conductivity for the 2 nm thick film are shown separately.

From the extrapolation $\sigma_1(\omega \to 0)$ we can estimate the dc resistivity. As visualized in Fig. 5, the scattering rate and resistivity of the 9 nm and the 5 nm films drop strongly as the temperature is reduced, but the drop is considerably enhanced for the 5 nm film. That is an unexpected result; scattering on topological rough interfaces should be temperature independent. The large influence of temperature on the scattering rate observed for thinner films is an indication that surface phonons play an important role in surface scattering. For $T < 200$ K phonons are frozen out and the scattering rate and resistivity remain almost constant with T for both samples.

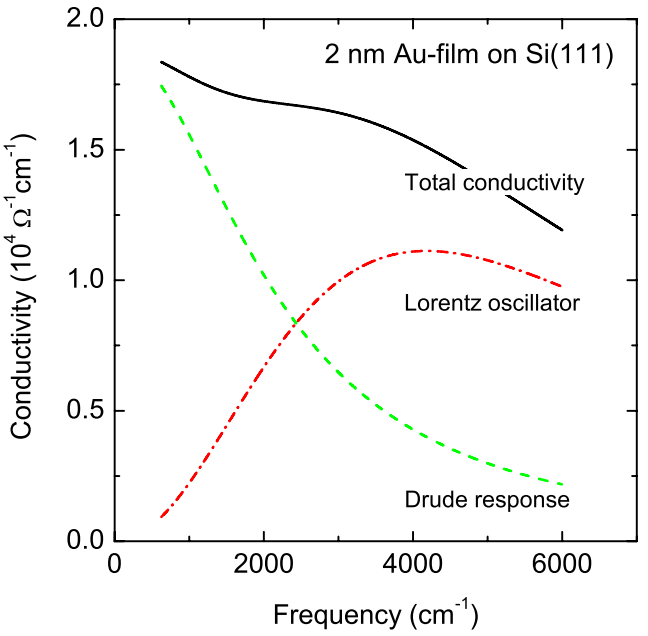

FIG. 4. (Color online) Total optical conductivity of a 2 nm thick Au film on Si at 300 K together with the two contributions: the Drude response of the free electrons at low frequencies and a broad Lorentz oscillator at higher frequencies.

B. Thin films at the percolation threshold

At a thickness of approximately 2 nm, the Au films undergo a metal-to-insulator transition which becomes already obvious by looking at the frequency and temperature-independent reflectivity (Fig. 6). For the 1 nm film the reflectivity below 4500 cm^{-1} changes its slope indicating a vanishing metallic behavior. At low frequencies the metallic contribution of the 3 nm and 2 nm film can still be analyzed by the Drude model with basically temperature-independent

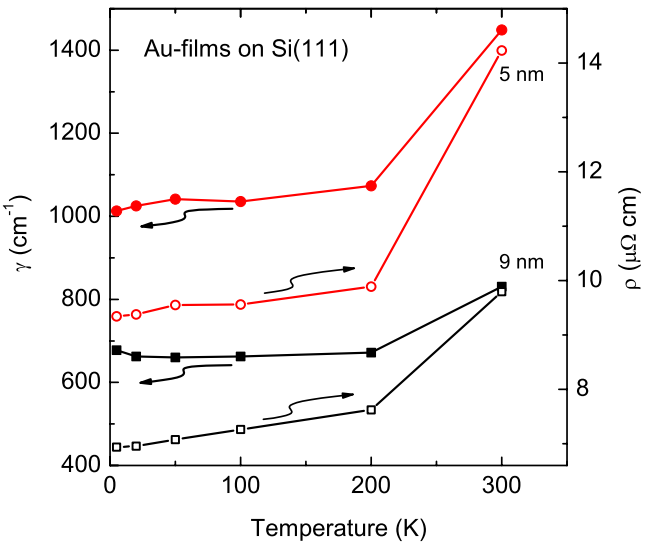

FIG. 5. (Color online) Temperature dependence of the scattering rate $\gamma = 1/(2\pi c\tau)$ and resistivity $\rho = 1/\sigma_1(\omega \to 0)$ for the 9 and 5 nm gold film. The full symbols correspond to the scattering rate (left scale), the open symbols correspond to the resistivity (right scale).

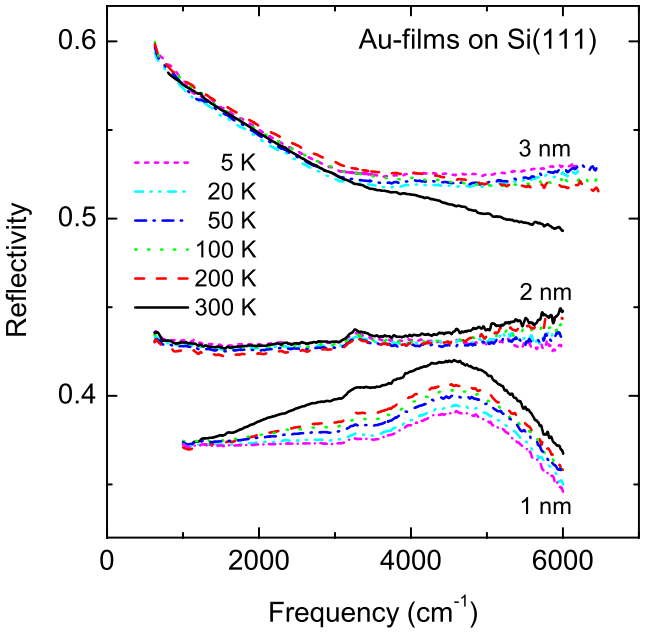

FIG. 6. (Color online) Frequency dependent reflectivity of three Au films (1, 2, and 3 nm) at the percolation threshold. Note the enlarged scale compared to Fig. 1.

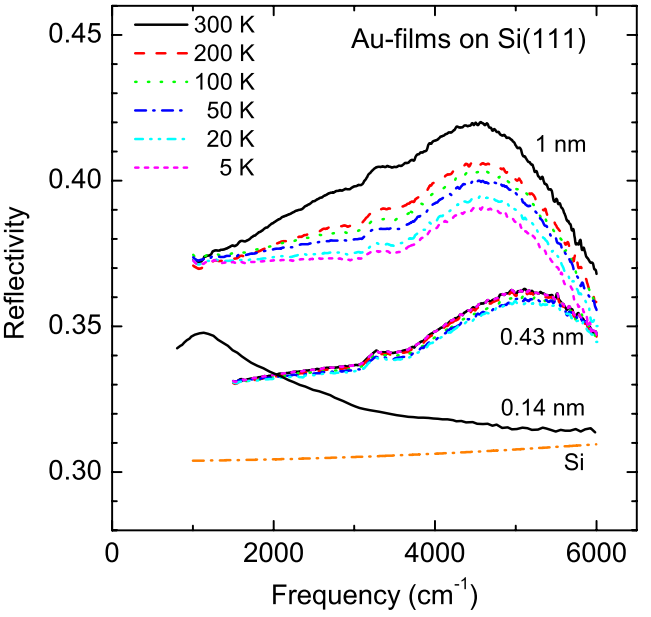

FIG. 7. (Color online) Reflectivity for ultrathin films below the percolation threshold. Here the temperature dependence is reversed compared to metallic transport. The dash dotted line corresponds to the reflectivity of bare silicon.

parameters. As summarized in Table I the values are in accord with the tendency observed for the 9 nm and 5 nm film: the scattering is even more dominated by grain boundaries, imperfections, and surface roughness but additionally the plasma frequency starts to drop for the thinner films. Around the percolation threshold not only the frequency dependence changes its slope but also the temperature dependence is reversed. Whereas the 3 nm film especially in the near infrared still shows a slight increase as the temperature is lowered down to 5 K, a tiny decrease is observed for the 2 nm film. This is much more pronounced for the 1 nm film, which shows clear indication for activated transport. All three films show in addition to their Drude component a contribution of a Lorentzian line. For the 2 nm thick film this Lorentzian oscillator at 4180 cm^{-1} makes the reflectivity nearly frequency independent. For the 1 nm film this oscillator is shifted to slightly higher frequencies and even more pronounced.

The most remarkable point is that for higher frequencies, i.e., in the near infrared, the optical reflectivity of films at the percolation threshold exceeds the one of thick films. Although it seems counterintuitive, it is a simple result of the fact that the reflectivity of a metal continuously drops with frequency, while it remains constant or even increases for films at and below the percolation threshold. There is an additional dielectric contribution to the electrodynamic response due to polarization effects: the isolated clusters interact capacitively.

C. Ultrathin films

Below the percolation threshold, i.e., for a thickness $d \leq 2$ nm, the temperature and frequency characteristics are inverted compared to a metal, as shown in Fig. 7. In addition, the reflectivity of bare silicon is displayed in the figure. For the monolayer corresponding to a nominal thickness of 0.14 nm, the optical reflectivity approaches the one of bare Si, except a strong excitation observed around 1100 cm^{-1} which we ascribe to localized surface excitations.

From our temperature-dependent optical experiments we can get information about the high-frequency transport mechanism of ultrathin gold films. In the near-infrared range the optical conductivity increases as the coverage is lowered (see Fig. 8). A strong and broad resonancelike feature around 4700 cm^{-1} dominates the conductivity for the 1 nm film. For the 2 nm and even for the 3 nm film the onset of a yet overdamped resonance at lower frequencies can be identified. This feature becomes more dominant and sharper as the metal clusters get further separated and smaller. It cannot be ascribed to plasmon excitations of individual metal clusters commonly found in the visible spectral range.[18,19] It is most likely due to a "Maxwell-Garnett resonance," which is known to shift with the area fraction of the substrate covered by metal.[20,21] Due to the high refractive index of our substrate this resonances are in the case of Si expected to be in the infrared.

When the temperature is reduced, the peak does not shift but the overall intensity of the infrared conductivity decreases. In Fig. 9 the logarithm of the optical conductivity at various frequencies is plotted as a function of inverse temperature. In this Arrhenius plot, no straight line can be extracted over a large temperature range, and thus we cannot identify a simple activated transport behavior from our optical data as suggested by Hill[15] for the dc conductivity.

IV. DISCUSSION

The dc resistivity of thin gold films has been investigated as a function of grain diameter and temperature by various

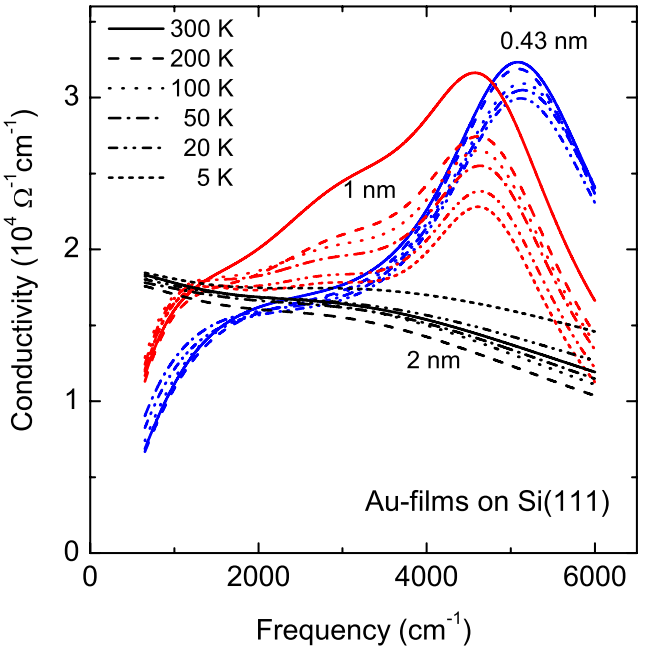

FIG. 8. (Color online) Conductivity spectra of ultrathin Au films as derived from reflectivity measurements (Figs. 6 and 7) with a nominal thickness of 2, 1, and 0.43 nm.

groups.[13,22] The granularity is varied by annealing the films and using different substrate materials; typically the film thickness is well above 10 nm. The importance of grain-boundary scattering as suggested by the model of Mayadas and Shatzkes[23] can explain most of the findings: a decrease in resistivity with increasing thickness and grain size, and the same linear temperature dependence above $T=50$ K. However, our data displayed in Fig. 5 obtained from the optical conductivity show a somewhat different behavior. Below 200 K the scattering rate and resistivity of the 5 nm and 9 nm films exhibit a similar but weaker temperature dependence compared to $T>200$ K. In the high-temperature range the 5 nm film exhibit a much steeper increase as T rises compared to the thicker films. Additional processes such as surface phonons have to be responsible for this behavior. Besides the Au surface, the interface between silicon and gold has to be taken into account. This interface was studied by a variety of methods which all came to the conclusion that there is some intermixing due to the high solubility of Au in Si.[16] This few monolayer thick intermixing region may become more important as the film thickness decreases.

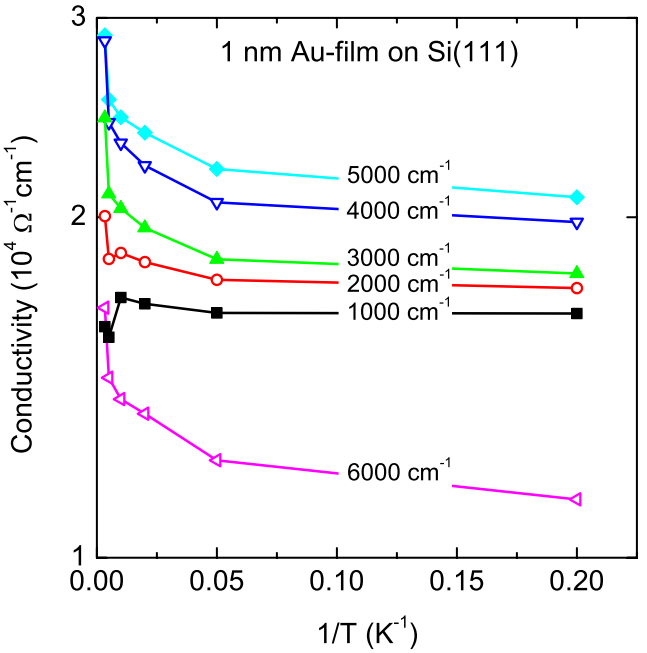

FIG. 9. (Color online) Arrhenius plot of the temperature dependence of the optical conductivity of a 1 nm Au film at different frequencies as indicated. No clear indication of a simple activated transport can be found.

We can fit the dominant midinfrared peak (cf. Figure 8) by a simple Lorentzian peak [Eq. (2)], centered around $\omega_0/2\pi c=4180$, 4733, and 5147 cm^{-1} for $d=2$, 1, and 0.43 nm, respectively. It gets obvious that with decreasing film thickness the peak shifts to higher frequencies. In a simple picture, these oscillatory contributions are ascribed to the capacitive coupling of the metallic clusters. Efros and Shkolvskii[24] considered such a situation and analyzed the critical behavior of conductivity and dielectric constant near the metal-insulator transition. They predicted a divergence of the dielectric constant at a certain filling fraction, which happens distinctively below the percolation threshold. Since the particle size and coverage is statistically distributed and interaction with the Si substrate has to be taken into account, a quantitative analysis of our data is not really possible in this regard.

Instead we want to consider the optical conductivity which remains after subtraction of the Lorentzian contribution from the measured conductivity spectra (Fig. 10). For thick films this should be the itinerant charge transport which becomes gradually localized as the metallic particles get increasingly disconnected and scattering at the boundaries is enhanced. Using the single-scattering approximation of the generalized Drude formula developed by Smith,[25] the real part of the conductivity is fitted by

$$\sigma_1(\omega) = \frac{\omega_p^2 \tau}{4\pi} \frac{1}{1+\omega^2\tau^2}\left[1 + s\frac{1-\omega^2\tau^2}{1+\omega^2\tau^2}\right]. \quad (3)$$

Here the second term describes the backscattering leading to some localization of the charge carriers. Accordingly the conductivity drops for $\omega \to 0$ as s decreases from 0 (regular Drude behavior) to −1 (complete localization with $\sigma_{dc}=0$). Below the percolation threshold no conduction path persists and the dc conductivity vanishes. In contrast to localization by impurities (Anderson localization) or electronic correlations (Mott localization), here we observe a geometrical localization by the formation of islands on a nanometer scale. Applying Eq. (3), we obtain $s=-1$ for the $d=0.14$ nm film. As the film thickness increases, backscattering becomes less important and the value of s changes to −0.84 and −0.71 for $d=0.43$ and 1 nm, respectively. In absence of the Lorentzian contribution the 2 nm film shows a Drude-type behavior ($s=0$) with very low effective carrier density and high scattering rate (cf. Table II). As one example for the temperature

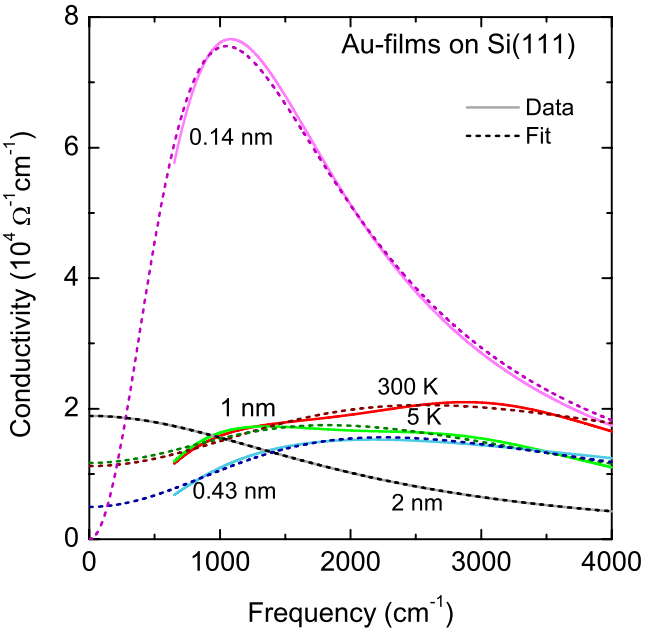

FIG. 10. (Color online) Fit of the low-frequency conductivity spectra by Eq. (3). The Lorentz contribution was subtracted to focus on the itinerant electrons. The dashed lines are the experimental data taken from Fig. 8; the solid lines correspond to the generalized Drude model which also takes backscattering into account.

dependence of the Drude-Smith parameters, we have listed for the 1 nm film also the 5 K values. In the framework of the model, not only the scattering rate and the plasma frequency become temperature dependent, but also the s parameter. In addition an extrapolation of the generalized Drude formula to $\omega \rightarrow 0$ leads to the strange result that the 1 nm as well as the 0.43 nm film exhibit a nonvanishing dc conductivity for films below the percolation threshold. In this context it becomes obvious that the applicability of Eq. (3) seems to be restricted and that the plasma frequency as well as the scattering rate loses their normal meaning. For the thinnest film (0.14 nm), for example, the plasma frequency in the generalized Drude description is higher than the bulk value.

At a coverage of one monolayer (0.14 nm), Au on Si(111)(7×7) forms a well ordered Si(111)-Au(6×6) reconstruction, which can be clearly identified by LEED. Beside the absence of the midinfrared peak, this well ordered surface shows an excitation at 1083 cm^{-1}, which we attribute to a transition between filled and empty surface states. This excitation was not identified by photoelectron spectroscopy until now and demonstrates that FTIR spectroscopy is a powerful complimentary technique for the characterization of metal monolayers.

TABLE II. Parameters obtained by fitting the low-frequency part of the conductivity of thin metal films after subtracting the oscillatory contribution, as described in the text. The Drude-Smith formula [Eq. (3)] contains an additional backscattering term, which is maximal for $s=-1$ and vanishes for $s=0$. The temperature is denoted by T, ω_p is the plasma frequency, $\gamma=1/(2\pi c\tau)$ the scattering rate.

Film thickness (nm)	T (K)	$\omega_p/2\pi c$ (10^4 cm^{-1})	γ (cm^{-1})	s
2	300	4.95	2165	0
1	5	6.95	2410	−0.65
1	300	8.65	3120	−0.71
0.43	300	6.79	2480	−0.84
0.14	300	9.25	1050	−1

V. CONCLUSION

Above the percolation threshold the optical behavior of Au films in the infrared spectral range can be described by the Drude model when classical size effects are considered. At the percolation threshold the optical response becomes frequency and temperature independent. Below the threshold the optical properties of ultrathin metal films are reversed; the reflectivity increases with frequency and decreases with temperature. Whereas the frequency dependence can in principle be described by a generalized Drude formalism, the temperature behavior cannot be fitted to a simple Arrhenius-type activated transport. For monolayers, we could identify infrared transitions between surface states located around 1100 cm^{-1}. To uncover the underlying physical processes leading to the observed high-frequency temperature dependence of the conductivity, further investigations on different metal-substrate systems around the percolation threshold are in progress.

ACKNOWLEDGMENT

We would like to thank N. Drichko for the valuable help during the optical experiments.

[1] H. E. Bennett and J. M. Bennett, in *Optical Properties and Electronic Structure of Metals and Alloys*, edited by F. Abelès (North-Holland, Amsterdam, 1966); J. M. Bennett and E. J. Ashley, Appl. Opt. **4**, 221 (1965); *Handbook of Optical Constants of Solids*, edited by E. D. Palik (Academic, Orlando, 1985).
[2] G. Fahsold, A. Bartel, O. Krauth, N. Magg, and A. Pucci, Phys. Rev. B **61**, 14108 (2000); G. Fahsold, M. Sinther, A. Priebe, S. Diez, and A. Pucci, *ibid.* **65**, 235408 (2002).
[3] M. Walther, D. G. Cooke, C. Sherstan, M. Hajar, M. R. Freeman, and F. A. Hegmann, Phys. Rev. B **76**, 125408 (2007).
[4] A. Pucci, F. Kost, G. Fahsold, and M. Jalochowski, Phys. Rev. B **74**, 125428 (2006).
[5] R. B. Laibowitz and Y. Gefen, Phys. Rev. Lett. **53**, 380 (1984).
[6] S. Kirkpatrick, Rev. Mod. Phys. **45**, 574 (1973).
[7] P. F. Henning, C. C. Homes, S. Maslov, G. L. Carr, D. N. Basov, B. Nikolic, and M. Strongin, Phys. Rev. Lett. **83**, 4880 (1999).
[8] J. C. M. Garnett, Philos. Trans. R. Soc. London **203**, 385 (1904).
[9] D. Bruggeman, Ann. Phys. **416**, 636 (1935).

[10] B. Gompf, J. Beister, T. Brandt, J. Pflaum, and M. Dressel, Opt. Lett. **32**, 1578 (2007).
[11] D. Bedeaux and J. Vlieger, *Optical Properties of Surfaces* (Imperial College, London, 2001).
[12] Y. Yagil, P. Gadenne, C. Julien, and G. Deutscher, Phys. Rev. B **46**, 2503 (1992).
[13] J. W. C. de Vries, Thin Solid Films **150**, 201 (1987).
[14] H. Marom and M. Eizenberg, J. Appl. Phys. **96**, 3319 (2004).
[15] R. M. Hill, Proc. R. Soc. London, Ser. A **309**, 377 (1969).
[16] G. LeLay, Surf. Sci. **132**, 169 (1983).
[17] M. Dressel and G. Grüner, *Electrodynamics of Solids* (Cambridge University Press, Cambridge, 2002).
[18] S. Link and M. A. El-Sayed, J. Phys. Chem. B **103**, 4212 (1999).
[19] L. B. Scaffardi, N. Pellegi, O. de Sanctis, and J. O. Tocho, Nanotechnology **16**, 158 (2005).
[20] R. Doremus, J. Appl. Phys. **37**, 2775 (1966).
[21] J. P. Marton and J. R. Lemon, Phys. Rev. B **4**, 271 (1971).
[22] G. Chen, P. Hui, K. Pita, P. Hing, and L. Kong, Appl. Phys. A: Mater. Sci. Process. **80**, 659 (2005).
[23] A. F. Mayadas and M. Shatzkes, Phys. Rev. B **1**, 1382 (1970).
[24] A. L. Efros and B. I. Shkolvskii, Phys. Status Solidi B **76**, 475 (1976).
[25] N. V. Smith, Phys. Rev. B **64**, 155106 (2001).